

POLARIZATION SIMULATIONS IN THE RHIC RUN 15 LATTICE *

F. Méot, H. Huang, Y. Luo, V. Ranjbar, G. Robert-Demolaize, S. White
 Collider-Accelerator Department, BNL, Upton, NY 11973, USA

Abstract

RHIC polarized proton Run 15 uses a new acceleration ramp optics, compared to RHIC Run 13 and earlier runs, in relation with electron-lens beam-beam compensation developments [1, 2]. The new optics induces different strengths in the depolarizing snake resonance sequence, from injection to top energy. As a consequence, polarization transport along the new ramp has been investigated, based on spin tracking simulations. Sample results are reported and discussed.

SIMULATED OPTICS

Main parameters of the *simplified* RHIC polarized proton optics considered for these simulations are given in Tab. 1, “Run 13” stands for the earlier optics, “Run 15” stands for the new one with betatron functions as displayed in Fig. 1. Tracking outcomes will be given for both cases,

Table 1: Optical Parameters in the Simulations

	Run 13	Run 15
Orbit length	m	3833.8452
γ_{tr}	23	23.5
Q_x	28.685	29.68
Q_y	29.673	30.67
Q'_x	1	2.3
Q'_y	1	2.2
<i>RHIC rings' snake 1 and snake 2 :</i>		
Spin rotation (deg.)	180, 180	
Axis angles (deg.)	+45, -45	

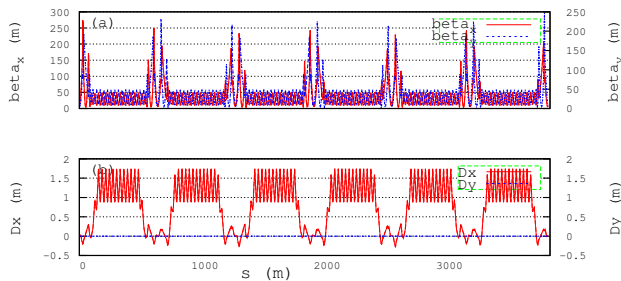


Figure 1: Betatron functions (maintained constant) in the ramp simulation, case of the new optics.

for comparison. In the simulations, optical functions are

maintained unchanged over the all ramp from injection, $E=23.8$ GeV, to collision, $E=100$ GeV (total energy). The $E \approx 33$ GeV optics is taken in the “Run 15” case, the location of the strongest intrinsic depolarizing resonance, $G\gamma = 93 - Q_y$. Higher energy optics was used in the “Run 13” case, however the intrinsic resonance strengths do not change much, in spite of the varying optics, during the ramp. The resonance sequence so obtained in the 23-100 GeV range is displayed in Fig. 2, Tab. 2 gives the strengths of the strongest ones.

RESONANCE STRENGTHS

Intrinsic resonance strengths for the old and for the new optics are displayed in Fig. 2. They have been computed in the thin-lens approximation, namely,

$$\frac{J_n^\pm}{\sqrt{\epsilon_y/\pi}} = \frac{1 + \gamma G}{4\pi} \sum_k \left\{ \begin{array}{l} \cos(\gamma G \alpha_k \pm \psi_{y,k}) + \\ i \sin(\gamma G \alpha_k \pm \psi_{y,k}) \end{array} \right\} (KL)_k \sqrt{\beta_{y,k}} \quad (1)$$

where the sum extends over the lattice quadrupoles

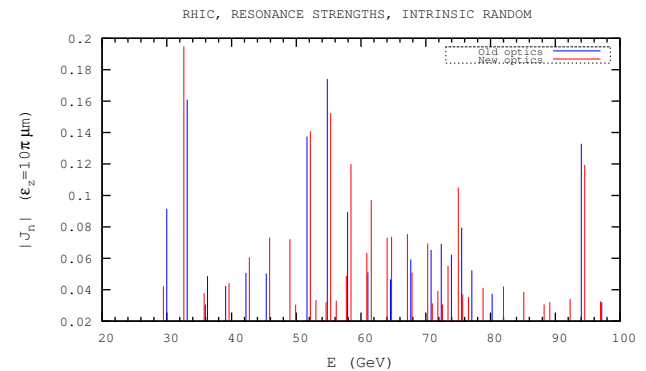


Figure 2: Resonance strengths in the simulation of the old and new optics.

Table 2: Strongest Resonances in the old and in the new Optics. Respectively, $Q_y = 29.673$ and $Q_y = 30.67$.

$n \pm Q_y$	E (GeV)	$ J_n(\epsilon_{y,\text{norm.}} = 10 \pi \mu\text{m}) $ Old optics	New optics
$93 - Q_y$	~ 33	0.161	0.195
$69 + Q_y$	~ 52	0.137	0.141
$75 + Q_y$	~ 55	0.174	0.152
$174 - Q_y$	~ 75	0.080	0.105
$150 + Q_y$	~ 94	0.133	0.120

(counter-rotating beam orbits are vertically separated at the

* Work supported by Brookhaven Science Associates, LLC under Contract No. DE-AC02-98CH10886 with the U.S. Department of Energy.

IPs during the ramp, by ± 5 mm about, the quadrupole feed-down so induced is neglected), and with ϵ_y/π the particle invariant and γ its Lorentz relativistic factor, $G = 1.7928$ the proton anomalous magnetic moment, and with respectively α_k , $\psi_{y,k}$ and $\beta_{y,k}$ the local orbit angle, vertical betatron phase and function at quadrupole index k . The \pm signs are for the resonances, respectively, $\gamma G \pm Q_y - n = 0$.

RAMPING

The RF conditions for the simulation of the ramp, for both the old and new optics, are given in Tab. 3. Note that $\dot{\gamma}$ is smaller by a factor of ~ 2 in reality, which means increased relative strength of the resonances, however with marginal resulting difference regarding polarization behavior, in the conditions of the present investigations.

Table 3: Parameters used in the Simulations

Orbit length	m	3833.8
RF harmonic		120
Peak voltage	kV	50
RF frequency	MHz	9.3776
Synchronous phase	deg	150
$\dot{\gamma}$	/s	2.0835

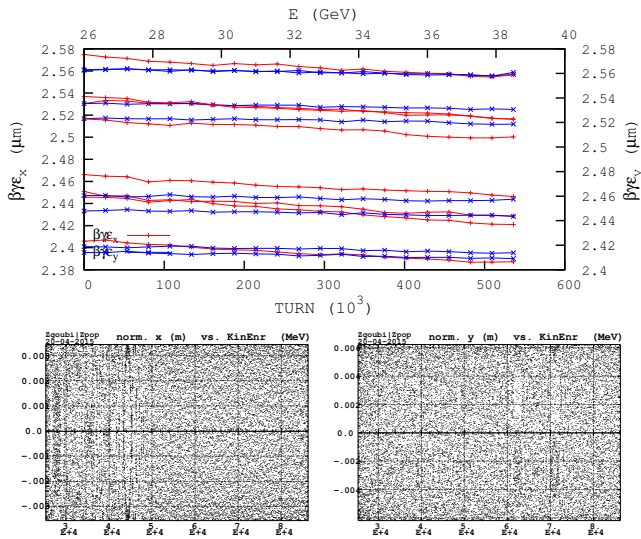


Figure 3: Observation at an IP. Top : normalized invariants over 500,000 turns. Bottom : turn-by-turn horizontal (left) and vertical (right) normalized excursions over 2 million turns.

The $\dot{\gamma} \approx 2.1 \text{ s}^{-1}$ rate considered means that the ramp takes 3 million turns. It is not a bad idea in these conditions to keep an eye on the symplecticity of the tracking (there is no symplectic tracking). This is illustrated in Fig. 3 which shows (i) the quasi-constant normalized invariants over 500 thousand turns, for sample particles launched on $\epsilon_x/\pi \approx \epsilon_y/\pi \approx 2.5 \mu\text{m}$, which is about the value of RHIC

rms beam emittance, and (ii) the horizontal and vertical normalized excursions ($x \times \sqrt{p/p_0}$ and $y \times \sqrt{p/p_0}$) of a particle launched on $\epsilon_x/\pi \approx \epsilon_y/\pi \approx 25 \mu\text{m}$ invariants over 2 million turns about, featuring constant extrema.

POLARIZATION TRANSPORT

Fig. 4 shows tracking results in the case of the old optics, 3 million turns about, namely, the evolution of the vertical spin component for 8 particles launched at 23.8 GeV, with their spin vertical, on initial invariants $\epsilon_x/\pi \approx \epsilon_y/\pi \approx 25 \mu\text{m}$ (i.e., 10 times the rms RHIC beam emittance) and with initial betatron phases evenly distributed over $[0, 2\pi]$. The vertical spin component S_y is observed at one of the two snakes of RHIC ring.

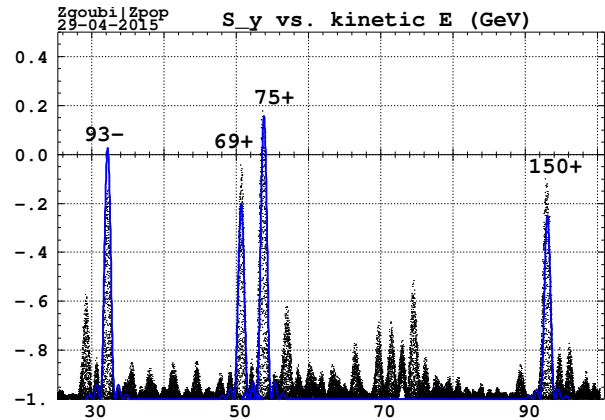


Figure 4: Old optics. Turn-by-turn S_y values, 8 particles on 10 rms invariants are plotted. Envelopes (blue curves) are from theory, Eq. 2.

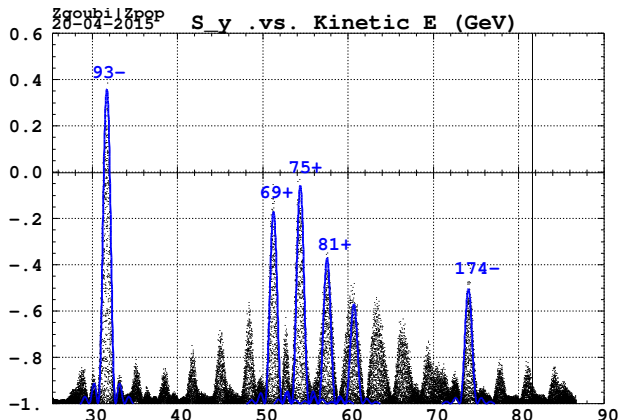


Figure 5: New optics. Turn-by-turn S_y values, 8 particles on 10 rms invariants are plotted. Envelopes (blue curves) are from theory.

Fig. 5 shows similar outcomes in the case of the new ramp optics. Further, not shown here, 8 particles launched with evenly distributed phases on 1 rms initial invariants, $\epsilon_x/\pi \approx \epsilon_y/\pi \approx 2.5 \mu\text{m}$, show/confirm similar preservation of polarization.

Content from this work may be used under the terms of the CC BY 3.0 licence (© 2015). Any distribution of this work must maintain attribution to the author(s), title of the work, publisher, and DOI.

All in all it can be seen that, even at such large invariant values (10 times RHIC *rms* beam emittance), the polarization over the ramp is preserved, showing a final average $\langle S_y \rangle$ comparable to its initial value, in % range from -1. Particles in RHIC beam are well within $\beta\gamma\epsilon_y/\pi \sim 25 \mu\text{m}$, hence no major depolarization effect is to be expected during the ramp from injection energy to 100 GeV collision energy, in the present working hypotheses.

Comparison with Theory

In passing, we compare the evolution of the vertical spin component with expectations from the isolated resonance model [4]. The vertical spin component across an isolated resonance is expected to fall within

$$\langle S_y \rangle = 1 - 8b^2(1 - b^2), \text{ with } b = \sin \frac{\pi \sqrt{\delta^2 + |J_n|^2}}{2} \quad (2)$$

with δ = distance to the resonance = $G\gamma_R - G\gamma$.

This equation is applied independently on some resonance amongst the strong ones, with strength from Tab. 2. Both the old and new optics, Figs. 4 and 5 (blue curves), show satisfactory agreement with these envelopes.

LATTICE INDEPENDENT TRACKING

We also performed extensive lattice independent particle tracking across the DEPOL [5] calculated spin resonances around strongest intrinsic spin resonance at $93 - Q_y$. The code integrates the T-BMT equation using a 4th order Magnus Gaussian quadrature integrator described in [6], and can integrate over an arbitrary set of spin resonances, where the snakes are added into the lattice as thin spin kicks [7].

Including the $93 - Q_y$ spin resonance we considered the five neighboring intrinsic spin resonances for 128 particles distributed evenly over an initial betatron phase at a fixed emittance (resonance strength). By scaling up and down the relative spin resonance strengths we could construct a predicted polarization response at different emittances. We began our particles on the initial ISF calculated via stroboscopic averaging and then determined the polarization loss by comparing the final spin state to the ISF at the final energy. For the nominal spin resonances the polarization aperture didn't show any significant loss beyond $100\pi\mu\text{m}$ for the several tunes looked at between 0.675-0.690. The introduction of imperfections equal to about 1.5 mm rms orbit error (particularly the one at $G\gamma = 62$) brought aperture down to 50π (see Fig. 6). The introduction of a strong coupled intrinsic spin resonance at $93 - Q_x$ equal to 0.066 at 10π reduced the polarization aperture down to 38π .

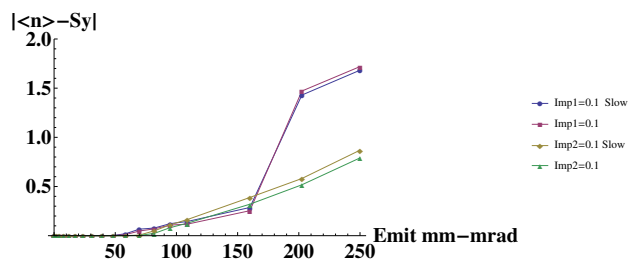


Figure 6: Polarization aperture with $Q_y = 0.675$ and considering the addition of imperfection resonances of 0.1 at $G\gamma = 62$ (Imp1) and $G\gamma = 63$ (Imp2). We consider response for both nominal (pp run) and slower ramp rate by 2.22 (p-Au run).

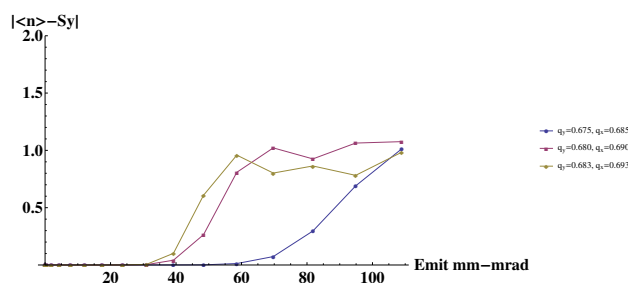


Figure 7: Polarization aperture at three different working points considering the addition of a single coupled intrinsic spin resonance at $93 - Q_x$ with a strength of 0.066 at $10\pi\mu\text{m}$ which is 33% of the primary $93 - Q_y$ spin resonance.

REFERENCES

- [1] V. Schoefer et al., RHIC polarized proton-proton operation at 100 GeV in Run 15, IPAC15, these proceedings.
- [2] S. White et al., Optics Solutions for pp operation with electron lenses at 100 GeV, C-AD Note C-A/AP/519, Brookhaven National Laboratory (2014)
- [3] The ray-tracing code Zgoubi, F. Méot, NIM-A 427 (1999) 353-356 ; <http://sourceforge.net/projects/zgoubi/>
- [4] S.Y. Lee, Spin dynamics and snakes in synchrotrons, World Scientific (1997).
- [5] E.D. Courant and R.D. Ruth, BNL 51270, 1980.
- [6] S. Blanes et. al. Physics Reports, 407, pp151 (2009)
- [7] V. H. Ranjbar Proceedings of Spin 2014 Beijing China (2014).